A Modified Adaptive Droop Control for Improved Load Sharing in Microgrids Considering DG Boundary Limits

Ahmed Rashwan
Faculty of Energy Engineering, Aswan University, Aswan, Egypt,
engrashwan@aswu.edu.eg

Abstract -

The focus of the paper is on addressing a crucial aspect of microgrid operation, namely the need for efficient load sharing. In microgrids that employ high angle droop control, achieving optimal load sharing can be challenging and can potentially lead to instability. To overcome this issue, the paper proposes a modified adaptive droop control technique that stabilizes the system while ensuring appropriate load sharing. The technique involves controlling each distributed generator converter separately using high angle droop gains and a droop approach that predicts grid characteristics such as voltage, frequency, and impedance angle and magnitude. Active and reactive power can be injected into the grid separately, and a suitable dynamic can be introduced independent of the grid impedance's magnitude and phase. This ensures that the system remains stable and performs optimally, even under varying load conditions. Furthermore, during the load sharing process, the DG units have the potential to reach their maximum limits, which can lead to the collapse of the microgrid. To address this issue, a control strategy is introduced in this paper to alleviate the overloading experienced by the microgrid's units. The proposed modified adaptive droop control loop was tested on a microgrid test system, and simulation results demonstrate the effectiveness of the technique in achieving optimal load sharing while maintaining system stability. Overall, the paper provides valuable insights into the design and implementation of control strategies for microgrids, which can enhance their performance and reliability.

Keywords: The adaptive droop control loop - Load sharing- Grid impedance - Distributed generator

1. INTRODUCTION

An autonomous microgrid is a self-sufficient energy system that operates independently from the larger centralized power grid. It is designed to generate, distribute, and store electricity at a local level, providing reliable and sustainable energy to a specific area or community [1]. With its advanced control systems and intelligent technologies, an autonomous microgrid can seamlessly integrate renewable energy sources such as solar panels and wind turbines, along with traditional sources like diesel generators, to ensure a stable and resilient power supply [1, 2]. This innovative solution not only increases energy efficiency but also reduces greenhouse gas emissions, making it a viable option for remote or off-grid locations. Furthermore, the autonomous nature of the microgrid allows it to disconnect from the main grid during power outages or emergencies, providing a vital lifeline for critical infrastructure, such as hospitals or emergency response centers. In a world where energy sustainability and resilience are paramount, autonomous microgrids offer a powerful solution to meet the evolving energy needs of the future.

Autonomous microgrids with power sharing capabilities and distributed generation (DG) play a significant role in revolutionizing the energy landscape. These microgrids offer a decentralized approach to energy generation and distribution by utilizing various sources of DG, such as solar panels, wind turbines, or small-scale generators. Power sharing in autonomous microgrids refers to the ability of different energy sources within the microgrid to share their excess power with other components or neighboring microgrids [3, 4]. This sharing can occur through advanced control systems that monitor the energy production and consumption within the microgrid, ensuring a balanced supply and demand. The integration of DG sources into an autonomous microgrid provides several benefits. Firstly, it reduces the reliance on traditional centralized power plants and the need for long-distance power transmission, resulting in lower transmission losses and improved overall energy efficiency. Moreover, the power sharing capabilities of autonomous microgrids enable the optimization of energy resources. For instance, if one source of DG is experiencing low energy production, the excess power from other sources can be redirected to compensate for the shortfall, ensuring a continuous and reliable electricity supply. This ability to share power enhances the stability and resilience of the microgrid, particularly during peak energy demand or unforeseen disruptions. Furthermore, power sharing in autonomous microgrids supports the concept of energy islands, where communities or facilities can operate independently from the main power grid. This autonomy helps in enhancing energy

ISSN: 2636 - 3712 (Printed Version)
ISSN: 2636 - 3720 (Online Version)

security, especially in remote areas or during emergencies when the main grid may be inaccessible or unreliable [5-7].

The increasing penetration of renewable energy sources in the power sector has led to a growing need for effective integration and control of these sources into the existing electrical grid. Power electronics devices, such as DC/AC converters, are playing a vital role in this process by regulating voltage stability in both islanded and grid-connected systems. In islanded systems, where communities or facilities operate independently from the main power grid, DC/AC converters are used to convert the direct current (DC) generated by renewable sources, such as solar panels or wind turbines, into alternating current (AC) suitable for consumption. These converters ensure that the voltage supplied to the local distribution grid remains stable, regardless of the fluctuating nature of renewable energy generation. Similarly, in grid-connected systems, where renewable energy sources are integrated into the main power grid, DC/AC converters known as voltage source inverters (VSIs) are employed. VSIs convert the DC power from renewable sources into AC power, which is synchronized and in phase with the grid's voltage. This synchronization, along with voltage regulation capabilities, helps maintain grid stability and allows for the seamless injection of renewable energy into the existing power infrastructure. The use of power electronics devices, such as DC/AC converters and VSIs, not only facilitates the integration of renewable energy sources but also provides additional benefits. These include improved power quality, enhanced grid reliability, and the ability to control and manage power flows effectively. Moreover, the flexible nature of power electronics devices enables the smooth integration of various renewable energy technologies and allows for the optimal use of available resources [8-10].

VSIs are considered the basic component in the DG applications because they do not need any external loops to maintain the synchronization. In addition, they can be connected in parallel with other inverters to create isolated or independent microgrids using frequency and voltage droops [11, 12]. Furthermore, ride-through capability and power equality capability are very essential issues in the modern power production systems which can be given by the control of the VSIs that make it practical solution [13]. The ability of the switching from voltage source to current source in case of working in the grid- connected mode is another merit of the VSIs. The imported and exported power to the flexibility of the microgrid to work in both isolated and grid-connected is considered a challenge to the VSIs control [14]. Droop control technique is considered a well-established control technique to supply the active and reactive power from the converter to the grid [15-21]. Droop control is depending mainly on varying the frequency and amplitude of the output voltage according to the grid requirements. However, some of the grid parameters are needed to be measured or estimated in the typical droop control technique to regulate the active and reactive power. Many research techniques in the literatures focus on the determination of the grid characteristics for both islanded or grid-connected mode [13-15, 22, 23].

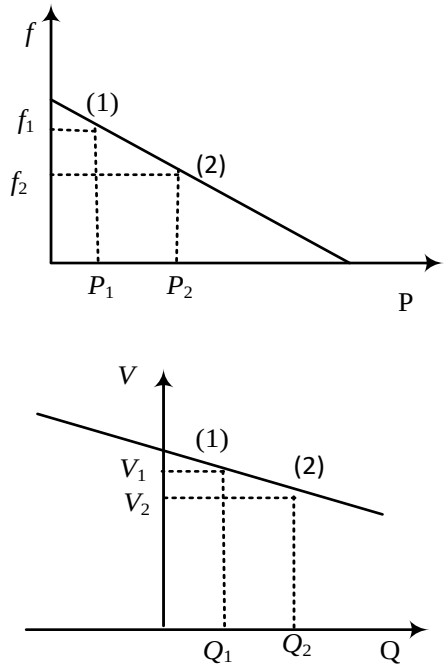

Fig.1 Power versus frequency droop and voltage versus reactive power droop.

In this paper, we introduce a control scheme based on the modified adaptive droop method. The droop control modifies the grid parameters using a grid impedance approximation technique, relying on measurements of voltage and current variations at the point of common coupling (PCC). The Voltage Source Inverter (VSI) seamlessly switches between grid-connected and islanded operation modes.

During the load sharing process, there is a potential risk of the DG units reaching their maximum limits, which can lead to the collapse of the microgrid. To address this issue, a control strategy is proposed in this paper to alleviate the overloading experienced by the microgrid's units.

The structure of this paper is as follows:

- Section II discusses the derivation of grid parameters using an estimation technique.

- In Section III, an adaptive droop control approach is presented, which decouples the flow of active and reactive power using predicted parameters.
- Section V showcases simulation results that demonstrate the viability of the suggested controller.
- Finally, Section VI provides the conclusions.

approach utilized in this paper. Such voltage and current phasors were observed using a second-order generalized integrator-based frequency locked loop (SOGI-FLL). The observation and analysis of voltage and current phasors were carried out utilizing a second-order generalized integrator-based frequency locked loop (SOGI-FLL). This advanced control technique allowed for accurate tracking and synchronization of the phasors within the electrical system. The SOGI-FLL employed a second-order integrator to ensure

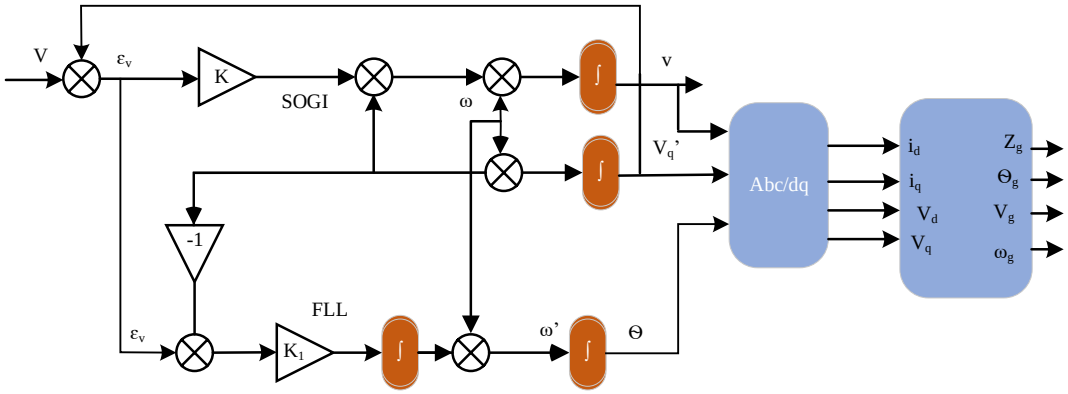

Fig. 2 Block diagram of the SOGI-FLL for grid parameter estimation algorithm.

2. GRID PARAMETERS CALCULATION METHOD

Multiple grid-forming sources face challenges due to minor frequency errors. However, these issues can be effectively resolved by employing a power vs. frequency droop function, as shown in Fig. 1. When the microgrid separates from the main grid, the voltage phase angles at each source undergo changes, leading to an apparent shift in the local frequency. By combining this frequency adjustment with an appropriate power alteration, each source can contribute its fair share of power. To incorporate a significant number of grid-forming sources into a microgrid, basic unity power factor controls are insufficient. It becomes essential to ensure voltage regulation for local reliability and stability. In the absence of local voltage control, systems with high penetrations of grid-forming sources may experience substantial circulating reactive currents between the sources. If the voltage set points have slight errors, these circulating currents can surpass the source ratings. To tackle this issue, a voltage vs. reactive power droop controller becomes necessary. This controller reduces the local voltage set point as the reactive power generated by the source becomes more capacitive. Conversely, as the reactive power becomes more inductive, the voltage set point is increased.

The voltage and current phasors between the VSI and the grid were processed at the PCC as part of the grid characterization

precise frequency detection and extraction. By continuously adjusting the loop parameters, it maintained a stable and reliable lock on the frequency of the system. This enabled the extraction of essential information regarding the voltage and current waveforms, such as their magnitudes, angles, and phase relationships. The utilization of the SOGI-FLL proved to be an effective and efficient method for monitoring and analyzing the behavior of the voltage and current phasors within the electrical system. The SOGI was implemented using two cascaded integrators operating in a closed loop, as illustrated in Fig. 2 [24, 25]. The grid monitoring system boasted key features such as high accuracy, low computational cost, and frequency adaptability [26, 27].

In addition to the grid parameters estimation, the mentioned SODI-FLL can be used to measure the current injected at the PCC from which the current phasor $I = i_d + ji_q$ can be calculated. Furthermore the SODI-FLL acts as harmonic filter on the measured current and voltage [28]. An accurate estimation of the current and voltage of the grid (V_g and I_g) at the fundamental frequency can be performed by using SODI-FLL. After detecting the grid current and voltage, a transformation to d–q reference frame has been performed to produce relevant current and voltage phasors.

A linear performance of the grid to which distributed generation are attached informs the method used to estimate the grid characteristics [29]. A power generator's PCC may therefore be

used to visualize the grid as a straightforward Thevenin circuit made up of a voltage Vg and grid impedance Z_g. Fig. 3 shows the relation between the current and the voltage at the PCC. The figure helps further clarify the impedance help detection method.

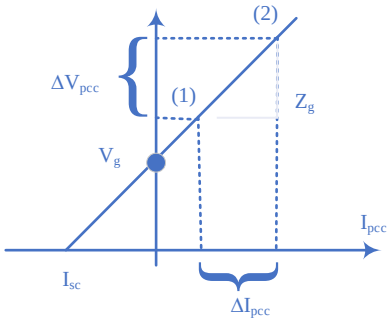

Fig. 3 The relation between the current and the voltage at the PCC.

As shown from Fig.2, the linear relation between the current and voltage at the PCC can help in the calculation of the grid impedance Z_g. By measurement the voltage droop ΔV_{pcc} and current droop ΔI_{pcc}, the grid impedance Z_g and grid voltage V_g can be calculated as follows:

$$\vec{Z}_g = Z_g \angle\theta_g = \frac{\Delta\vec{V}_{pcc}}{\Delta\vec{I}_{pcc}} = \frac{\vec{V}_1 - \vec{V}_2}{\vec{I}_1 - \vec{I}_2} \quad (1)$$

$$\vec{V}_g = V_g \angle\emptyset_g = \vec{V}_{pcc(i)} - \vec{Z}_g\vec{I}_{pcc(i)} = \frac{\overrightarrow{\vec{I}_1\vec{V}_2} - \overrightarrow{\vec{I}_2\vec{V}_1}}{\vec{I}_1 - \vec{I}_2} \quad (2)$$

There are fundamental clues to the foundation of the grid impedance detection methods [28] through [30-33]. In this paper, the active power (P) and reactive power (Q) variations produced by a grid-connected converter with a droop controller were used to predict the grid characteristics. The precision of the PCC's online measurements of the voltage and current phasors, which were carried out on the basis of the SOGI-FLL, served as the basis of this estimation approach. The technique employed in this study to determine the grid parameters is depicted in Fig. 1. It must be noted that with each variation in the grid parameters, the predicted angle and magnitude values of the grid voltage impedance, as well as their voltage and frequency, are momentarily incorrect. Consequently, as seen in Fig. 1, just the monitored voltage v was used to execute the FLL block, and the angle was determined by integrating the voltage frequency.

3. THE PROPOSED ADAPTIVE DROOP CONTROL

The proposed adaptive droop controller is defined in this section. It is based on the grid parameters identification's algorithm. The active and reactive power can be injected to the grid accurately. From the PCC, the active power P and reactive power Q injected into the grid by the VSI can be calculated as follows:

$$P = \frac{1}{Z_g}\left[\left(EV_g\cos\emptyset - V_g^2\right)\cos\theta_g + EV_g\sin\emptyset\sin\theta_g\right] \quad (3)$$

$$Q = \frac{1}{Z_g}\left[\left(EV_g\cos\emptyset - V_g^2\right)\sin\theta_g - EV_g\sin\emptyset\cos\theta_g\right] \quad (4)$$

where

E, ∅: The VSI magnitude and phase, respectively;

V_g: The grid voltage.

It can be observed that both equations are dependent on the grid impedance Z_g, θ_g. Thus, we can transform these equations to a form independent of the grid impedance magnitude and phase, i.e., P_c and Q_c, as follows:

$$P_c = Z_g\left(P\sin\theta_g - Q\cos\theta_g\right) \quad (5)$$

$$Q_c = Z_g\left(P\cos\theta_g - Q\sin\theta_g\right) \quad (6)$$

By substituting Eqs. (3) and (4) into Eqs. (5) and (6),

$$P_c = EV_g\sin\emptyset \quad (7)$$

$$Q_c = EV_g\cos\emptyset - V_g^2 \quad (8)$$

It is observed from Eq.7 and Eq.8 that the injected active power P_c is dependent on the phase angle ∅ and the injected reactive power Q_c is depending on the voltage difference between E and V_g. The adaptive droop control uses these variables (i.e., P_c and Q_c) to inject the active and reactive power to the grid.

The objective of the droop control was to inject active and reactive power (i.e., P* and Q*). The block diagram of the adaptive droop control is shown in Fig. 4. The angle ∅ and voltage magnitude E can be obtained from Eqs. (3) and (4) as follows:

$$\emptyset = -G_p(s)Z_g\left[(P - P^*)\sin\theta_g - (Q - Q^*)\cos\theta_g\right] \quad (9)$$

$$E = E^* - G_q(s)Z_g\left[(P - P^*)\cos\theta_g + (Q - Q^*)\sin\theta_g\right] \quad (10)$$

where E^* is the voltage reference's magnitude that can be estimated from the grid voltage V_g. The compensator transfer functions G_p, G_q can be defined as follows:

$$G_p(s) = \frac{m_i + m_p s + m_d s^2}{s} \quad (11)$$

$$G_q(s) = \frac{n_i + n_p s}{s} \quad (12)$$

Where;

m_i: Integral droop constant

m_p: Proportional droop constant

m_d: Derivative droop constant

n_i: Integral amplitude droop

n_i: Derivative amplitude droop

Equation (12) represents the transfer function of the compensator controller denoted as $G_q(s)$. Its type is Proportional-Integral-Derivative (PID) controllers.

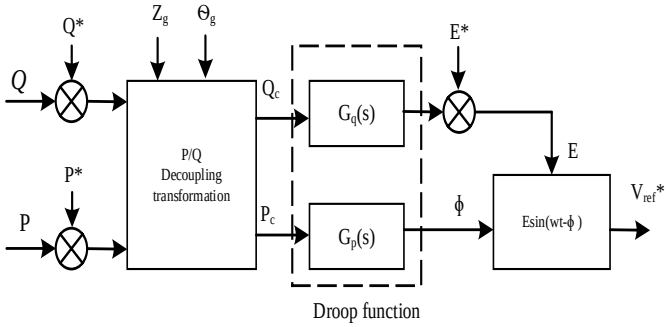

Fig. 4 The adaptive droop control block diagram.

The adaptive droop control method is a technique commonly used in power systems for regulating and controlling the operation of distributed energy resources (DERs). It offers several advantages and disadvantages, which are discussed below.

1. Improved stability: The adaptive droop control method enhances the stability of the system by adjusting the droop slope based on the system conditions. This allows for better regulation of voltage and frequency fluctuations.
2. Enhanced power sharing: By dynamically adapting the droop settings, the adaptive droop control method ensures a balanced power flow among distributed energy resources, resulting in optimal power sharing.
3. Flexibility in different operating conditions: The method can adapt to varying load conditions and grid configurations, making it suitable for different scenarios and improving overall system performance.
4. Reduced communication requirements: The adaptive droop control method relies less on communication infrastructure compared to centralized control methods, reducing dependencies and costs.

Disadvantages

1. Complexity: Implementing adaptive droop control requires more complex algorithms and control strategies compared to traditional droop control methods. This complexity can lead to increased system deployment and maintenance costs.
2. Parameter tuning: Adaptive droop control algorithms require accurate parameter tuning to ensure optimal performance. This process can be time-consuming and challenging, requiring expertise and careful calibration.
3. Limited scalability: As the system size increases and the number of DERs grows, the effectiveness of adaptive droop control may diminish. It may struggle to handle large-scale integration or face challenges in achieving precise sharing of power.

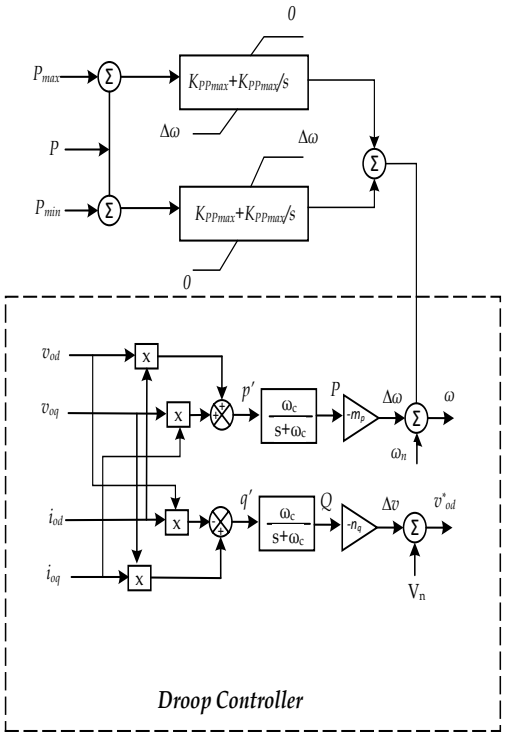

Fig. 5 DG boundary control technique.

4. CONTROL STRUCTURE

In Fig. 5, a control technique is depicted wherein the surplus load from one source is seamlessly transferred to the other without the need for communication. This technique relies on the utilization of power equations for two Distributed Generation (DG) units. In the event that one of the DGs reaches its maximum load capacity, such as DG1 (P_1), the controller illustrated in Fig. 5 will initiate a frequency reduction.

$$P_1 = \frac{V_1^2}{Z_{11}}\sin\alpha_{11} + \frac{V_1V_2}{Z_{12}}\sin(\delta_{12} - \alpha_{12}) \quad (13)$$

$$P_2 = \frac{V_2^2}{Z_{22}}\sin\alpha_{22} + \frac{V_1V_2}{Z_{12}}\sin(\delta_{12} + \alpha_{12}) \quad (14)$$

$$\delta_{12} = \int(\omega_1 - \omega_1)dt \quad (15)$$

By decreasing the frequency, the phase difference (δ_{12}) between the two sources increases, resulting in a decrease in the output power according to Eq. 15. This process continues until a steady-state point is reached, ensuring effective load redistribution between the DG units.

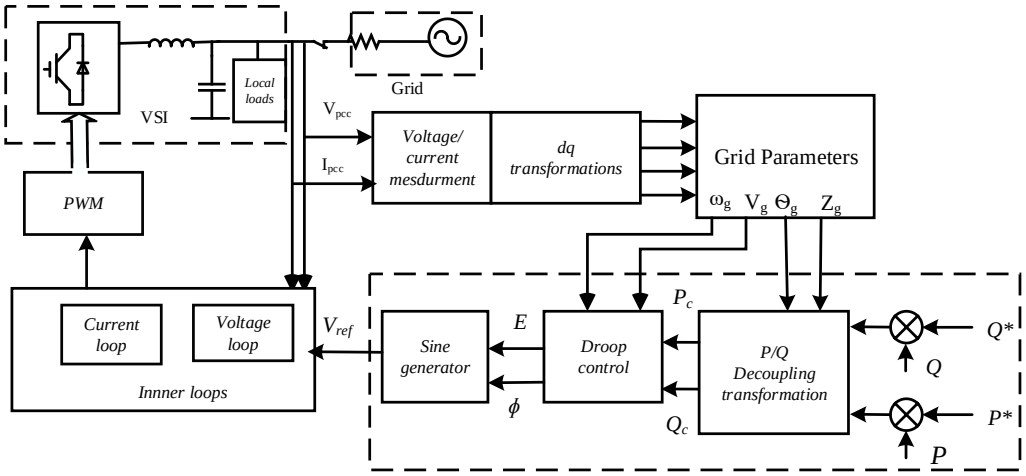

Fig. 6 The proposed adaptive droop control block diagram.

The suggested block design of the entire control system for the Voltage Source Inverter (VSI) converter is presented in Figure 6. This comprehensive design incorporates various control loops that have been discussed earlier in the context of the system. The control system includes multiple control loops responsible for regulating different aspects of the VSI converter's operation. The internal control loops specifically focus on maintaining precise control over the inverter's output voltage and output current. These internal control loops play a crucial role in ensuring the stability, accuracy, and desired performance of the VSI converter. By carefully monitoring and adjusting the output voltage and current, the control system enables the VSI converter to meet the requirements and demands of the connected load or grid. The suggested block design provides a structured and systematic approach to controlling the VSI converter, enabling efficient and reliable power conversion. The voltage, frequency, and grid impedance's magnitude and angle (V_g, ω_g, Z_g, and θ_g, respectively) may all be estimated using the SOGI-FLL loop and a related method. The adaptive droop controller uses these parameters to inject the necessary active and reactive power into the grid from the VSI. The calculation of the grid impedance can also aid in the identification of the islanded mode. The VSI is in island mode if Z_g is more than 1.75 or varies by more than 0.5 in 5 s. In scenarios where islanding occurs unexpectedly or is not planned, the detection of islanding becomes crucial to facilitate a seamless transition between the grid-connected and islanding modes. Islanding detection refers to the process of identifying when a distributed generation (DG) system becomes electrically isolated from the main grid and operates in islanding mode. This detection mechanism plays a vital role in ensuring the safety and stability of the overall power system.

The VSI delivers the local load as soon as the islanding mode is activated. By disconnecting the bypass switch, the VSI must begin synchronizing with the grid's phase, frequency, and amplitude when it is available. Achieving the synchronization of frequency and phase was accomplished by the output of the multiplication of the quadrature component of the VSI and grid voltage. Then, the output is processed through low-pass filter before sending it to the phase control loop (PCL). The rms voltage error between the VSI and the grid voltages must be calculated and proceeds by PI controller before passed to control loop to change the voltage amplitude. The VSI will therefore be synced with the grid after several line cycles, and the bypass can link the VSI and grid. At this point, the grid may be given the required P and Q.

5. RESULTS

In order to validate the effectiveness and viability of the suggested control approach, extensive simulations were conducted. The proposed controller was tested using appropriate simulation techniques on a single-phase Voltage

Source Inverter (VSI) system. The simulations incorporated the control parameters and system parameters outlined in Table I. The VSI was modeled using ideal semiconductor switch blocks to accurately represent its behavior. The single-line diagram of the system under study is depicted in Fig. 7. The system configuration consisted of two distribution generators, namely DG1 and DG2. Additionally, a switchable load was incorporated into the system to demonstrate and evaluate the efficacy of the proposed control technique. The simulations allowed for a comprehensive analysis of the control system's

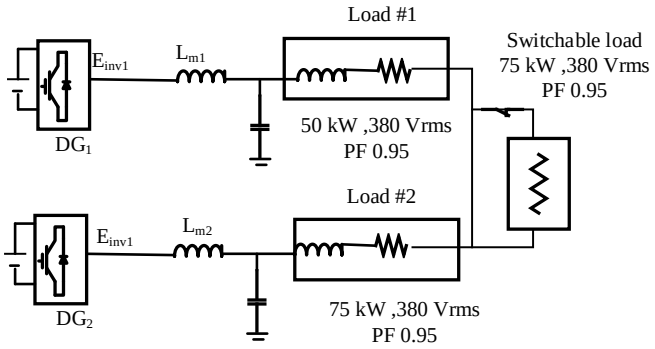

Fig. 7 Single line diagram of the studied microgrid.

response to various operating conditions, load variations, and grid disturbances. The results obtained from these simulations provided valuable insights into the viability and effectiveness of the suggested control approach for the VSI system.

The results are shown in the figures describe the steady state results of a test system that was used to evaluate the effectiveness of a proposed control technique in achieving optimal load distribution in microgrids. The test system was subjected to a step change in the load power at t=0.5s. This observation suggests that the proposed control technique is effective in regulating the voltage and reactive power output of the system. In Figure 7, the injected active and reactive power of the system is depicted, comparing the performance of conventional techniques with the proposed technique. Prior to t=0.5s, the load demand was expected to be evenly shared between the two Distributed Generators (DGs), and their respective dc-link voltages were maintained at 1000 V. However, at t=0.5s, an additional 75 kW load was introduced into the microgrid. The graph illustrates the response of the system under both the conventional and proposed techniques. It allows us to analyze the effectiveness of the proposed technique in handling the sudden increase in load. By comparing the active and reactive power injection curves, we can assess the performance of the system under different control strategies. The conventional techniques refer to the existing control methods employed before the proposed technique was implemented. These conventional techniques may include basic power sharing algorithms or other control strategies that were in place prior to the proposed improvement. On the other hand, the proposed technique refers to the new control approach introduced for the system. It aims to optimize the load sharing between the DGs and maintain stable operation during the addition of the 75 kW load. By examining the graph, we can observe and analyze the response of the system to the load change. It provides insights into how well the conventional techniques and the proposed technique handle the additional load and adjust the active and reactive power injections accordingly. This comparison helps in evaluating the effectiveness and efficiency of the proposed technique in achieving improved load sharing, voltage regulation, and overall system performance when faced with sudden changes in load demand The results show that the proposed adaptive droop control technique quickly reached a steady state within 0.1s, indicating good dynamic response. The output active power and reactive power of each inverter were well regulated, demonstrating the effectiveness of the proposed control technique in achieving optimal load distribution. Fig.8 shows the frequency of the two inverters, which settled to their nominal value (i.e., 60 Hz) after the step change. This outcome indicates that the proposed control technique is effective in regulating the frequency of the system. This results demonstrates that the proposed control technique is effective in regulating the voltage of the system, which is essential for ensuring proper functioning of the loads. Finally, Fig.10 and Fig.11 show the three-phase voltages and current injected to the loads, respectively.

The simulation results considering the boundary limits of the Distributed Generation (DG) units are presented in Fig. 11. The sudden increase in load by 30 kW is taken into account. In Fig. 11(a), the output of DG1 rises from 5 kW to 20 kW, and DG2's output increases abruptly from 55 kW to 70 kW following the load change. However, DG2 has reached its maximum capacity of 60 kW, triggering the activation of the maximum overload control technique. As depicted in Fig. 11(b), both frequency commands f_1 and f_2 initially decrease in accordance with the P vs. f droop. When DG2's output exceeds 60 kW, f_2 reduces at a faster rate compared to f_1 due to the activation of the overload mitigation control. In Fig. 11(c), the phase difference δ_{12} increases from -3.3° to -2.1° as a result of the variations in f_1 and f_2. With the increase in δ_{12}, the excess load from DG2 autonomously transfers to DG1 in less than 200 ms. Finally, as a result of the overload mitigation control, the power flow is redistributed, with DG2 outputting 60 kW and DG1 outputting 30 kW. Throughout this process, both DG1 and DG2 maintain their grid-forming characteristics, ensuring the load voltage remains constant, as illustrated in Fig. 11(d).

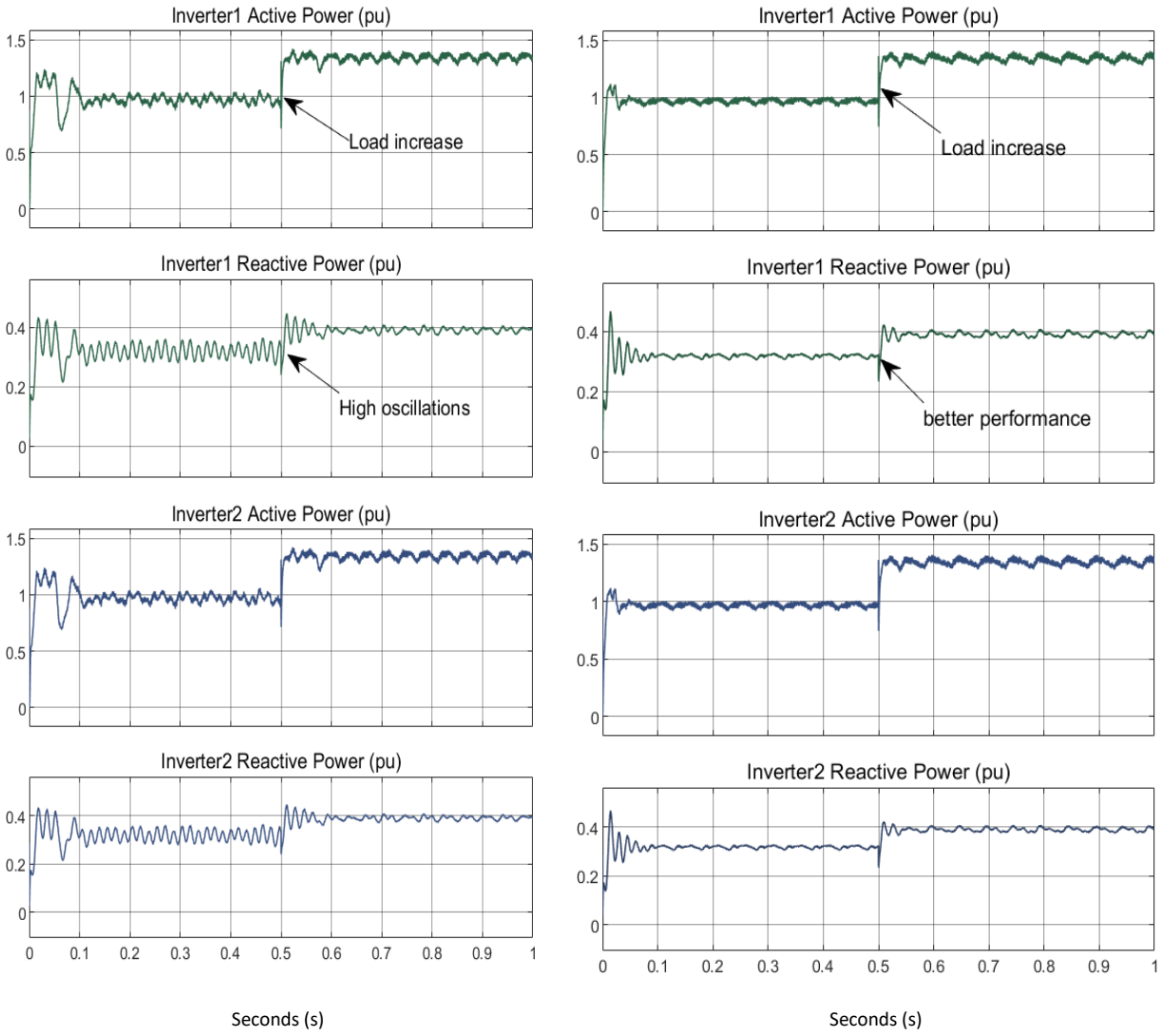

(a) power of inverters 1 and 2 of the conventional droop control.

(b) power of inverters 1 and 2 of the proposed droop control.

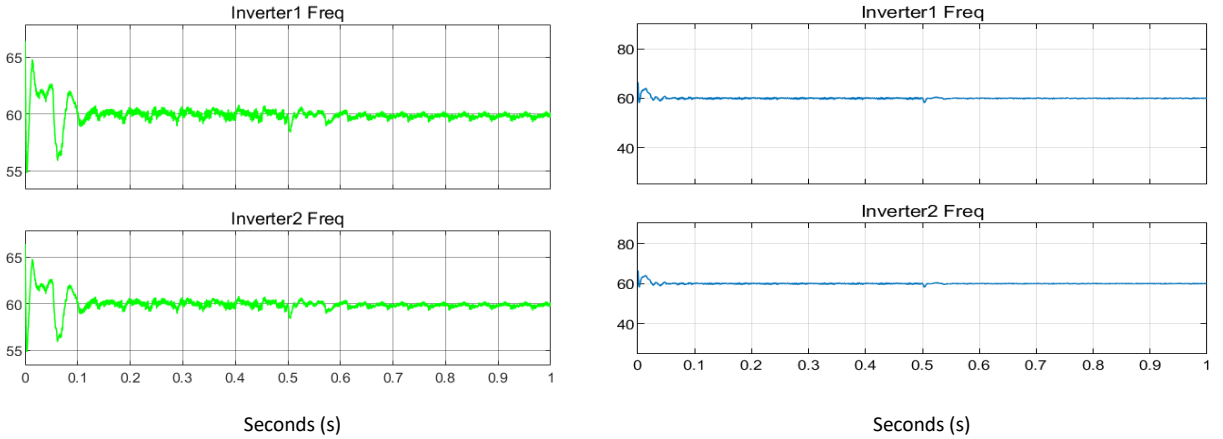

(c) Frequencies of inverters 1 and 2 of the conventional droop control [16].

(d) Frequencies of inverters 1 and 2 of the proposed droop control.

Fig. 8. Comparison between conventional and proposed methods

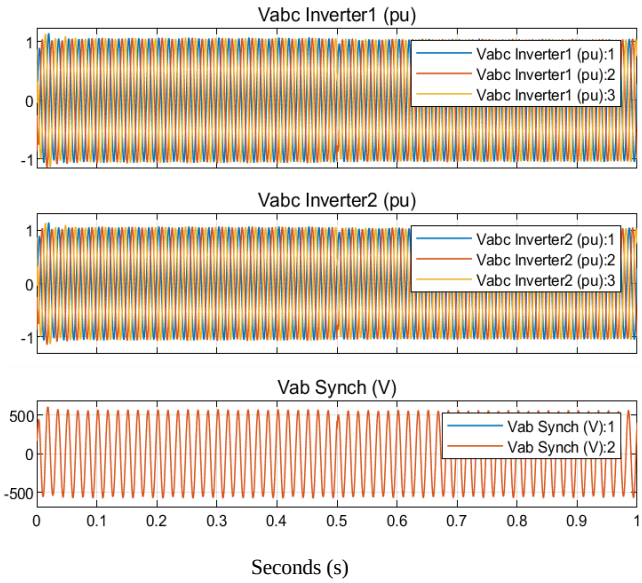

Fig. 9 Three-phase voltages of inverters 1 and 2.

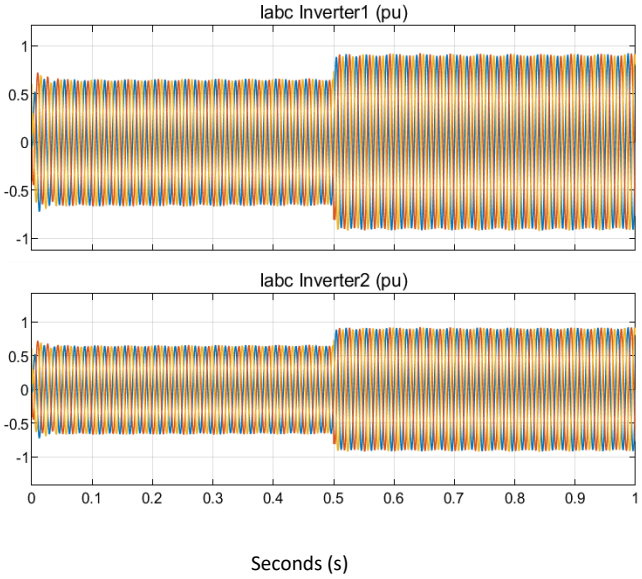

Fig. 10 Three-phase currents of inverters 1 and 2.

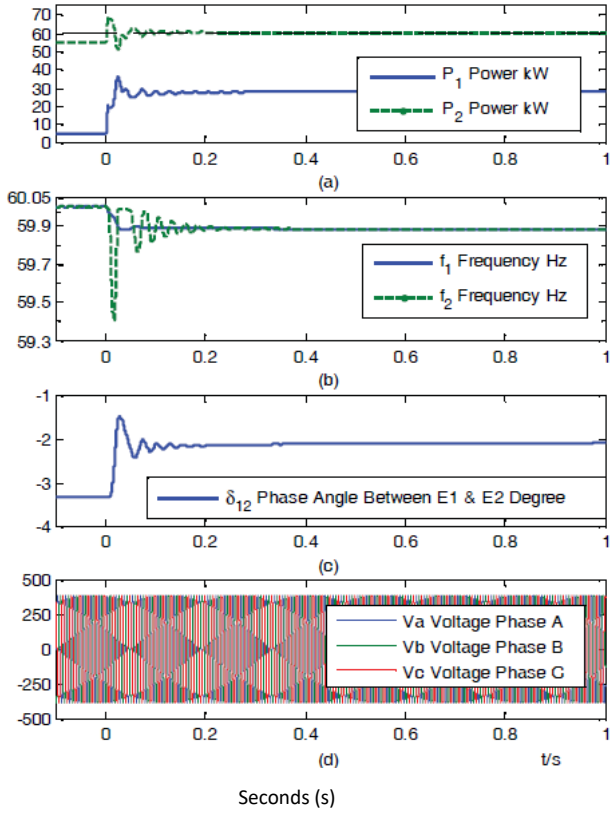

Fig. 11 The boundary mechanism simulation for the two DGs.

6. CONCLUSION

In this study, a novel control approach is introduced for a Voltage Source Inverter (VSI) that demonstrates effective operation in both islanding and grid-connected modes. When the VSI is connected to the grid, it successfully provides the required active and reactive power. The control system comprises two key components. Firstly, an estimation technique is utilized to accurately determine important grid parameters, such as amplitude, frequency, impedance magnitude, and phase. This estimation enables the system to acquire crucial information about the grid. Secondly, a droop control method is employed to separately inject active and reactive power into the grid, utilizing the estimated grid parameters. By incorporating these features, the proposed droop control system achieves precise regulation of both active (P) and reactive (Q) power, effectively closing the control loop. The feedback variables obtained from the estimator play a vital role in distinguishing the system dynamics from the grid parameters. The results of the study substantiate the effectiveness of the proposed control strategy in achieving precise regulation of DG VSIs for microgrid applications.

Appendix

Table I. System parameters

Parameter	Symbol	Value
Voltage grid	V_g	311 V
DC source	V_{dc}	1000 V
Frequency grid	ω^*	60 Hz
Resistance of Z_g	R_g	2 Ω
Inductance of Z_g	L_g	3 mH
Grid impedance magnitude	Z_g	2.3 Ω
Inverter impedance	L_m	0.2 mH
Grid impedance angle	θ_g	20.8°
Integral droop constant	m_i	0.0018
Proportional droop constant	m_p	0.00005
Derivative droop constant	m_d	7.10
Integral amplitude droop	n_i	0.15
Derivative amplitude droop	n_i	0.0004

References

[1] C. Zhong, H. Li, Y. Zhou, Y. Lv, J. Chen, and Y. Li, "Virtual synchronous generator of PV generation without energy storage for frequency support in autonomous microgrid," *International Journal of Electrical Power & Energy Systems*, vol. 134, p. 107343, 2022.

[2] M. Roslan, M. Hannan, P. J. Ker, and M. Uddin, "Microgrid control methods toward achieving sustainable energy management," *Applied Energy*, vol. 240, pp. 583-607, 2019.

[3] S. Rizvi and A. Abu-Siada, "A Review on Active-Power-Sharing Techniques for Microgrids," *Energies*, vol. 16, no. 13, p. 5175, 2023.

[4] S. Fazal, M. E. Haque, M. T. Arif, A. Gargoom, and A. M. T. Oo, "Grid integration impacts and control strategies for renewable based microgrid," *Sustainable Energy Technologies and Assessments*, vol. 56, p. 103069, 2023.

[5] L. Chen, Y. Wang, X. Lu, T. Zheng, J. Wang, and S. Mei, "Resilient active power sharing in autonomous microgrids using pinning-consensus-based distributed control," *IEEE Transactions on Smart Grid*, vol. 10, no. 6, pp. 6802-6811, 2019.

[6] D. Zhao, C. Zhang, Y. Sun, S. Li, B. Sun, and Y. Li, "Distributed robust frequency restoration and active power sharing for autonomous microgrids with event-triggered strategy," *IEEE Transactions on Smart Grid*, vol. 12, no. 5, pp. 3819-3834, 2021.

[7] F.-S. Pai and S.-J. Huang, "A detection algorithm for islanding-prevention of dispersed consumer-owned storage and generating units," *IEEE Transactions on Energy Conversion*, vol. 16, no. 4, pp. 346-351, 2001.

[8] M. C. Chandorkar, D. M. Divan, and R. Adapa, "Control of parallel connected inverters in standalone AC supply systems," *IEEE transactions on industry applications*, vol. 29, no. 1, pp. 136-143, 1993.

[9] S. Barsali, M. Ceraolo, P. Pelacchi, and D. Poli, "Control techniques of dispersed generators to improve the continuity of electricity supply," in *2002 IEEE Power Engineering Society Winter Meeting. Conference Proceedings (Cat. No. 02CH37309)*, 2002, vol. 2: IEEE, pp. 789-794.

[10] W. S. Ediriweera and N. Lidula, "Design and protection of microgrid clusters: A comprehensive review," *AIMS Energy*, vol. 10, no. 3, pp. 375-411, 2022.

[11] S. H. N. Kouakeuo *et al.*, "Internal characterization of magnetic cores, comparison to finite element simulations: a route for dimensioning and condition monitoring," *IEEE Transactions on Instrumentation and Measurement*, 2022.

[12] R. Teodorescu and F. Blaabjerg, "Flexible control of small wind turbines with grid failure detection operating in stand-alone and grid-connected mode," *IEEE transactions on power electronics*, vol. 19, no. 5, pp. 1323-1332, 2004.

[13] E. Buraimoh, A. O. Aluko, O. E. Oni, and I. E. Davidson, "Decentralized Virtual Impedance-Conventional Droop Control for Power Sharing for Inverter-Based Distributed Energy Resources of a Microgrid," *Energies*, vol. 15, no. 12, p. 4439, 2022.

[14] D.-H. Dam and H.-H. Lee, "A power distributed control method for proportional load power sharing and bus voltage restoration in a DC microgrid," *IEEE transactions on industry applications*, vol. 54, no. 4, pp. 3616-3625, 2018.

[15] J. C. Vasquez, J. M. Guerrero, A. Luna, P. Rodríguez, and R. Teodorescu, "Adaptive droop control applied to voltage-source inverters operating in grid-connected and islanded modes," *IEEE transactions on industrial electronics*, vol. 56, no. 10, pp. 4088-4096, 2009.

[16] S. Ferahtia, A. Djeroui, H. Rezk, A. Chouder, A. Houari, and M. Machmoum, "Adaptive Droop based Control Strategy for DC Microgrid Including Multiple Batteries Energy Storage Systems," *Journal of Energy Storage*, vol. 48, p. 103983, 2022.

[17] B. Fan *et al.*, "A Novel Droop Control Strategy of Reactive Power Sharing Based on Adaptive Virtual

Impedance in Microgrids," *IEEE Transactions on Industrial Electronics*, vol. 69, no. 11, pp. 11335-11347, 2021.

[18] L. Zhang, H. Zheng, Q. Hu, B. Su, and L. Lyu, "An adaptive droop control strategy for islanded microgrid based on improved particle swarm optimization," *IEEE Access*, vol. 8, pp. 3579-3593, 2019.

[19] A. Mellit, M. Benghanem, A. H. Arab, and A. Guessoum, "An adaptive artificial neural network model for sizing stand-alone photovoltaic systems: application for isolated sites in Algeria," *Renewable energy*, vol. 30, no. 10, pp. 1501-1524, 2005.

[20] W. Xing, H. Wang, L. Lu, X. Han, K. Sun, and M. Ouyang, "An adaptive virtual inertia control strategy for distributed battery energy storage system in microgrids," *Energy*, vol. 233, p. 121155, 2021.

[21] H.-A. Trinh, H.-V.-A. Truong, and K. K. Ahn, "Development of fuzzy-adaptive control based energy management strategy for PEM fuel cell hybrid tramway system," *Applied Sciences*, vol. 12, no. 8, p. 3880, 2022.

[22] S. Zhou, J. Liu, Y. Zhang, and X. Cheng, "More Generalized Resonant Controllers for the Current Regulation of Power Electronics Converters in Stationary Referecne Frame," in *2018 IEEE Energy Conversion Congress and Exposition (ECCE)*, 2018: IEEE, pp. 3076-3082.

[23] J. Wang, J. Wang, and X. Luo, "Novel PLL for power converters under unbalanced and distorted grid conditions," *The Journal of Engineering*, vol. 2019, no. 17, pp. 3895-3899, 2019.

[24] H. Wang, C. Buchhagen, and J. Sun, "Methods to aggregate turbine and network impedance for wind farm resonance analysis," *IET Renewable Power Generation*, vol. 14, no. 8, pp. 1304-1311, 2020.

[25] D. K. Alves, R. L. Ribeiro, F. B. Costa, and T. O. A. Rocha, "Real-time wavelet-based grid impedance estimation method," *IEEE Transactions on Industrial Electronics*, vol. 66, no. 10, pp. 8263-8265, 2018.

[26] R. A. Fantino, C. A. Busada, and J. A. Solsona, "Grid Impedance Estimation by Measuring Only the Current Injected to the Grid by a VSI With $ LCL $ Filter," *IEEE Transactions on Industrial Electronics*, vol. 68, no. 3, pp. 1841-1850, 2020.

[27] D. Li, T. Wang, W. Pan, X. Ding, and J. Gong, "A comprehensive review of improving power quality using active power filters," *Electric Power Systems Research*, vol. 199, p. 107389, 2021.

[28] S. Khan, X. Zhang, B. M. Khan, H. Ali, H. Zaman, and M. Saad, "AC and DC impedance extraction for 3-phase and 9-phase diode rectifiers utilizing improved average mathematical models," *Energies*, vol. 11, no. 3, p. 550, 2018.

[29] M. K. De Meerendre, E. Prieto-Araujo, K. H. Ahmed, O. Gomis-Bellmunt, L. Xu, and A. Egea-Àlvarez, "Review of local network impedance estimation techniques," *IEEE access*, vol. 8, pp. 213647-213661, 2020.

[30] Y. Zhan, Y. Guo, J. Zhu, L. Li, B. Yang, and B. Liang, "A review on mitigation technologies of low frequency current ripple injected into fuel cell and a case study," *International Journal of Hydrogen Energy*, vol. 45, no. 46, pp. 25167-25190, 2020.

[31] X. Hu, D.-W. Chen, H. Zhang, D.-Q. Jia, Y. Li, and F. Zhang, "A novel control strategy for parallel operation of multi-inverters in low-voltage microgrids," *Energy Reports*, vol. 6, pp. 1212-1220, 2020.

[32] R. Wang, Q. Sun, D. Ma, and Z. Liu, "The small-signal stability analysis of the droop-controlled converter in electromagnetic timescale," *IEEE Transactions on Sustainable Energy*, vol. 10, no. 3, pp. 1459-1469, 2019.

[33] M. R. Shakarami and R. Sedaghati, "Design of Direct Power Control for Distributed Generation Units in Multi-Bus Microgrid," *Journal of Electrical and Electronics Engineering*, vol. 11, no. 1, pp. 27-32, 2018.